

No evidence of a metal-insulator transition in dense hot aluminum: A first-principles study

Pier Luigi Silvestrelli

Istituto Nazionale per la Fisica della Materia and Dipartimento di Fisica "G. Galilei," Università di Padova, via Marzolo 8, I-35131 Padova, Italy

(Received 29 June 1999)

Structural and electronic properties of dense hot aluminum are studied by *ab initio* simulation using the molecular-dynamics scheme based on finite-temperature density-functional theory. The electrical conductivity of the system is computed from the Kubo-Greenwood formula for the optical conductivity. This study covers the density range $\rho = 1.4\text{--}2.0$ g/cm³, at temperatures $T = 1000\text{--}8000$ K. Within this range of densities and temperatures, analysis of data obtained from a recent experiment on laser-heated aluminum seems to indicate that the system undergoes a metal-insulator transition characterized by a dramatic decrease of the electrical conductivity that assumes values that differ by at least an order of magnitude from current theoretical predictions. The results of the present simulation show no evidence of such a transition. Rather dense hot aluminum appears to behave like a standard liquid metal. [S0163-1829(99)16647-5]

I. INTRODUCTION

Aluminum is widely used in technical applications. Therefore, its properties, particularly its electrical conductivity, are of considerable interest. Recently, Mostovych and Chan¹ succeeded in preparing aluminum in a regime (characterized by a density $\rho \sim 0.5\text{--}1.0\rho_{\text{solid}}$, and a temperature $T \sim 4000\text{--}9000$ K), which is intermediate between the ordered solid and liquid phases, and the highly disordered gas phase, under conditions of thermal equilibrium and at sufficiently high pressure (30–100 kbar) to be well above the predicted critical point pressure and boiling curve. In this transitional regime, dense hot matter is typically degenerate and strongly coupled; moreover experimental data are limited. Using time-resolved laser probes to measure the reflectivity and adopting a free-electron Drude conduction model, Mostovych and Chan infer that the electrical conductivity of the sample assumes values that are sharply below those of liquid aluminum and differ by at least an order of magnitude from current theoretical predictions. In particular, they find that the conductivity falls dramatically as aluminum is heated above ~ 4500 K (~ 0.4 eV), substantially deviating from extrapolations of liquid-metal theory obtained from the known behavior of liquid aluminum near the melting point. Interestingly, the conductivity falls to levels consistent with a state of “minimum metallic conductivity” and the metal-insulator transition.² Moreover, most of the drop occurs in a narrow temperature range between 4000 and 6000 K (~ 0.35 to 0.55 eV), with little additional change at higher temperatures. This behavior is in strong contrast to that observed in short-pulse experiments (in which thermal equilibrium between laser-heated electrons and ions is not assured) and also to that obtained in recent theoretical predictions^{3–5} based on generalized Ziman models and strongly coupled plasma theory.

If confirmed this phenomenon would be particularly interesting and intriguing from a theoretical point of view. In fact it would represent the observation of a metal-insulator transition in a metal characterized by a value of the density that is not much lower than that of the liquid at normal condi-

tions. Hence, the transition would be mainly driven by the temperature increase. Unfortunately, in their paper, Mostovych and Chan proposed no plausible physical mechanism leading to such a peculiar transition, which is expected to be different from the metal-insulator transition, observed, for instance, in expanded alkali metals and usually described with the Mott-Hubbard model.⁶ Since the conductivity data reported by Mostovych and Chan differ from the other estimates by at least an order of magnitude, the discrepancy could be attributed to the failure of some of the assumptions used in the interpretation of the experimental data. For instance, the sharp drop in the reflectivity (and consequently in the conductivity) could result from gradients at the Al-SiO₂ interface used in the experiment, although Mostovych and Chan¹ claim that this is unlikely. Moreover, the electrical conductivity is obtained by the measured reflectivity assuming a Drude conduction model whose validity in the whole range of measurements is in principle questionable.

In order to shed some light on this issue, I have performed *ab initio* simulations of liquid aluminum, at the same conditions of the experiment, using a code specifically developed to deal with systems characterized by finite electronic temperature and computing the electrical conductivity from the Kubo-Greenwood⁷ formula, which is able to circumvent the limitations of the Ziman approach. Analysis of the simulation results does not support the existence of a metal-insulator transition in dense hot aluminum. In fact the aluminum fluid behaves like a standard liquid metal at all the densities and temperatures considered, and the electrical conductivity does not exhibit any sudden drop to values lower than the minimum metallic conductivity level.

The outline of the paper is as follows. In Sec. II, I present the algorithm used and provide computational details, with particular emphasis on the method employed for the calculation of the electrical conductivity. In Sec. III, the results of the simulations are reported and discussed. Finally, some conclusions are drawn in Sec. IV.

II. METHOD

Ab initio molecular-dynamics (MD) simulation of metals poses a variety of technical problems for which different

TABLE I. Basic parameters for liquid aluminum at the conditions considered in the simulations. r_s/a_0 is the electron sphere radius parameter; T_F is the Fermi temperature, and Γ_c is the ion coupling parameter (assuming $Z=3$).

ρ (g/cm ³)	T (K)	r_s/a_0	T/T_F	Γ_c
2.0	1000	2.291	0.009	860.0
2.0	5000	2.291	0.045	172.0
1.7	5000	2.419	0.050	162.9
1.4	5000	2.581	0.057	152.7
1.4	8000	2.581	0.092	95.5

methods, with different solutions, have been proposed. Here, I follow the approach of Alavi *et al.*,⁸ which is based on a new formulation of the finite-temperature Mermin density-functional theory (DFT).⁹ This technique¹⁰ is particularly suitable for studying electronic properties of metallic systems at high temperatures since a self-consistent electronic-structure calculation is performed at each MD step and the effect of thermal electronic excitations is consistently incorporated using fractionally occupied states. The same method has been already successfully applied to study dense hot hydrogen,^{8,11} liquid sodium,¹² the metal-insulator transition in metal-molten salt solutions,¹³ laser-heated silicon¹⁴ and graphite,¹⁵ and oxidation processes on transition metals.¹⁶

Simulations have been performed, at constant volumes, in a periodically repeated simple cubic box containing $N=72$ aluminum atoms. With this value of N , using the Γ point ($k=0$) only to sample the Brillouin Zone (BZ), the Fermi level is located in the middle of a quasidegenerate set of energy levels. Therefore, no large, unphysical energy gap is present between conduction and valence bands. The size of the cubic box has been varied to reproduce three different densities ($\rho=1.4, 1.7$, and 2.0 g/cm³) which span the density range considered in the experiment of Mostovych and Chan.¹ For all these density values simulations have been performed at a temperature of 5000 K. Moreover, in order to check the effect of the temperature alone (by keeping the density constant), for $\rho=2.0$ g/cm³ a simulation at 1000 K, and for $\rho=1.4$ g/cm³ a shorter simulation at 8000 K, have also been performed. In plasma physics language all the calculations were carried out (see Table I) deep in the quantum domain ($T/T_F \ll 1$, where T_F is the Fermi temperature of the fully degenerate noninteracting electron gas), and in the ‘‘strong-coupling regime.’’ In fact the ion coupling parameter, $\Gamma_c = (Ze)^2 / (ak_b T)$, where $a = [3V_b / (4\pi N)]^{1/3}$ is the ion-sphere radius ($V_b = L^3$ is the simulation box volume), which represents the ratio of the mean potential energy to the mean kinetic energy, was always $\gg 1$.

The interaction between ions and valence electrons has been modeled using a norm-conserving pseudopotential¹⁷ with s and p nonlocality. The electronic orbitals were expanded in plane waves with a cutoff of 16 Ry. This Al pseudopotential has been successfully used in *ab initio* simulations¹⁸ of solid and molten aluminum at the melting point. As an additional test, aluminum dimer properties in the ground state have been computed. In Table II the equilibrium distance and the vibrational frequency of Al₂ are reported. As can be seen, the comparison with the experimental data is satisfactory.

For a given configuration of ions, the electronic density

$n(\mathbf{r})$ has been computed by minimizing the free energy functional F of the electron gas. This is defined as

$$F = \Omega + \mu N_e + E_{II}, \quad (1)$$

where

$$\Omega[n(\mathbf{r})] = -\frac{2}{\beta} \ln \det(1 + e^{-\beta(\mathcal{H} - \mu)}) - \int d\mathbf{r} n(\mathbf{r}) \left[\frac{\phi(\mathbf{r})}{2} + \frac{\delta\Omega_{xc}}{\delta n(\mathbf{r})} \right] + \Omega_{xc}, \quad (2)$$

$\beta = 1/(k_B T)$ is the inverse electronic temperature, μ is the chemical potential, N_e is the total number of valence electrons, $\mathcal{H} = -(1/2)\nabla^2 + V(\mathbf{r})$ is the one electron Hamiltonian with the effective potential $V(\mathbf{r}) = \sum_I V_{ei}(\mathbf{r} - R_I) + \phi(\mathbf{r}) + \delta\Omega_{xc}/\delta n(\mathbf{r})$, $\phi(\mathbf{r})$ is the Hartree potential of an electron gas of density $n(\mathbf{r})$, Ω_{xc} the exchange-correlation energy in the local-density approximation (LDA), and E_{II} the classical Coulomb energy of the ions. The functional Ω_{xc} is approximated by its $T=0$ expression, since its finite-temperature corrections are negligible²⁰ at the temperatures and the electronic densities of the system studied. F reproduces the exact finite-temperature density of the Mermin functional⁹ and was self-consistently optimized for each ionic configuration. As in the experiment of Mostovych and Chan,¹ thermodynamic equilibrium between electrons and ions has been assumed in the simulations, so that the electronic temperature and the average ionic temperature were equal. Efficient diagonalization of the one electron Hamiltonian has been performed by means of a variant²¹ of the Lanczos algorithm, which allows optimal use of a good guess of the initial wavefunction. The electronic density is expressed in terms of the single-particle orbitals

TABLE II. Equilibrium distance d and vibrational frequency ω of Al₂, as obtained by *ab initio* simulation, using a normconserving pseudopotential, the local spin-density approximation of DFT with a plane-wave energy cutoff of 16 Ry, and a simple cubic unit cell of 30 a.u. Comparison is made with experimental data.

	d (Å)	ω (cm ⁻¹)
Simulation	2.71	247
Experiment ^a	2.70	284

^aReference 19.

$$n(\mathbf{r}) = \sum_i f_i |\psi_i(\mathbf{r})|^2, \quad (3)$$

where f_i are the Fermi-Dirac occupation numbers, $f_i = (e^{\beta(E_i - \mu)} + 1)^{-1}$, and the ionic forces are calculated using the Hellmann-Feynman theorem. The ionic degrees of freedom have been integrated using a time step of 50 a.u. (~ 1.2 fs). In the first part of each simulation the system has been equilibrated, for ~ 1 ps, at a given average ionic temperature, starting from a disordered initial configuration. Then production runs of ~ 1 ps have been performed in which structural and electronic properties of the system have been computed. Simulations have been carried out using the Γ point only to sample the BZ. However, for a selected set of ionic configurations, at different temperatures and densities, the one electron Hamiltonian has also been diagonalized using a different, more thorough, k -point sampling (with 8 k points) of the BZ, according to the prescription of Monkhorst and Pack.²² In fact, a previous study¹² of liquid sodium showed that, while the Γ point only sampling of the BZ is generally adequate to reproduce structural properties, it can be much less accurate for the electronic ones, particularly the electrical conductivity.

Calculations of dc electrical conductivity for dense systems are typically based on variations of the Ziman formula.²³ The Ziman theory is based on a quasi-free-electron approximation and makes use of the Boltzmann approach to transport (it represents the simplest solution to the transport equation). While this method is generally adequate for liquid metals near the melting point, a more general theoretical approach is needed for more highly disordered systems at elevated temperatures. Some recent generalized calculations exist. Rinker³ used an ‘‘average atom’’ partial-wave formulation of the Ziman theory: the electron states and interaction cross sections are calculated self consistently but the ion structure factor is taken from independent calculations for one-component plasmas. Perrot and Dharma-wardana⁴ used a density-functional, neutral pseudoatom model in which the ion-electron interactions and the structure factor are calculated self consistently within the framework of DFT and the ‘‘average atom’’ model. This generalization of the Ziman approach aims at extending the applicability of the method from the usual weak-isolated-scatterer limit to the regime of strong multiple scatterers. Both these calculations predict conductivities which are at least an order of magnitude larger than those reported by Mostovych and Chan.¹ In contrast, the calculations of Ichimaru *et al.*⁵ for hydrogen plasmas predict (using $Z=3$, that is the valence of aluminum) conductivities that are about an order of magnitude lower than in the experiment of Mostovych and Chan; this latter behavior is understandable since, in this case, the validity range of the calculations is limited to lower coupling strengths than are found in the experiment.

It has to be stressed that all the mentioned theoretical calculations made various assumptions about the electron-ion, ion-ion, electron-electron interaction, and/or the ionic structure, which make their general validity difficult to assess. Electron localization and details of the ionic structure can play an important role, particularly in the vicinity of a metal-insulator transition. Therefore, a method that calculates conductivities quantitatively, treats electron-ion and

electron-electron interactions quantum mechanically and that makes no *a priori* assumptions about ion-ion forces and the ionic structure is highly desirable. Such a method is represented by *ab initio* MD,^{8,24} in which both thermal (ionic) and electronic structure effects are incorporated at a high level of accuracy, and no empirical parameters are involved in the calculations. This *ab initio* approach allows in principle to circumvent¹² the limitations of the Ziman formula; in fact the interactions are computed from first-principles calculations performed on the fly as the simulation proceeds. One can, therefore, obtain the electronic excitation spectrum. Using this information the electrical conductivity can be calculated by means of the Kubo-Greenwood approach,⁷ as it has been done in many other *ab initio* simulations.^{12-15,25} This in principle straightforward procedure allows to transcend the weak-scattering limit of the Ziman formula. In fact the Kubo-Greenwood formula⁷ is a very general formulation for the conductivity: it contains electron-phonon and (as far as it is allowed by the use of DFT-LDA) electron-electron scattering. In this approach, the electrical conductivity σ can be obtained by extrapolating to zero frequency the optical conductivity:

$$\sigma = \sigma(0) = \lim_{\omega \rightarrow 0} \sigma(\omega), \quad (4)$$

with $\sigma(\omega)$ computed as a configurational average of

$$\sigma(\omega, R_I) = \frac{2\pi e^2}{3m^2\omega} \frac{1}{V_b} \sum_{i,j} (f_i - f_j) |\langle \psi_i | \hat{p} | \psi_j \rangle|^2 \delta(E_j - E_i - \hbar\omega), \quad (5)$$

where e and m are the electronic charge and mass, \hat{p} is the momentum operator and ψ_i , E_i , are the electronic DFT eigenstates and eigenvalues, calculated for the ionic configuration $\{R_I\}$, at a single k point (for instance the Γ point) of the BZ. The generalization of Eq. (5) to more than one k -vector sampling is straightforward

$$\sigma(\omega, R_I) = \sum_{\mathbf{k}} \sigma(\omega, R_I, \mathbf{k}) \cdot W(\mathbf{k}), \quad (6)$$

where $\sigma(\omega, R_I, \mathbf{k})$ is defined by Eq. (5), with the eigenstates and the eigenvalues computed at \mathbf{k} , and $W(\mathbf{k})$ is the weight of the point \mathbf{k} . Of course, the use of the single-particle DFT states and eigenvalues, instead of the true many-body eigenfunctions and eigenvalues, introduces an approximation in the calculation of σ . Due to the finite-size discretization of the eigenvalue spectrum, in practical applications $\sigma(\omega, R_I)$ is computed for a finite set of frequencies ($\omega_1, \omega_2, \dots, \omega_l, \dots$) by averaging over a small frequency range $\Delta\omega$

$$\sigma(\omega_l, R_I) \approx \frac{1}{\Delta\omega} \int_{\omega_l - \Delta\omega/2}^{\omega_l + \Delta\omega/2} \sigma(\omega, R_I) d\omega. \quad (7)$$

The value of $\Delta\omega$ must be carefully chosen. In fact it has to be large enough to assure that a sufficient number of electronic levels contribute, and, at the same time, small enough to allow a good resolution. A value of $\Delta\omega = 0.2$ eV was found to be adequate for liquid aluminum. Since a limited number of excited states have been included in the calcula-

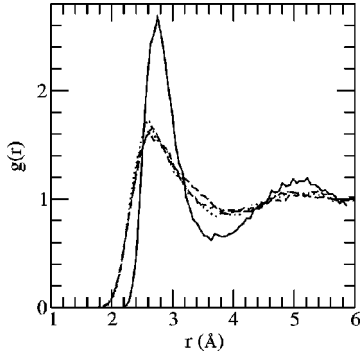


FIG. 1. Pair correlation function $g(r)$ of liquid aluminum at different densities and temperatures: $\rho=2.0$ g/cm³, $T=1000$ K (solid line); $\rho=2.0$ g/cm³, $T=5000$ K (dotted line); $\rho=1.7$ g/cm³, $T=5000$ K (dashed line); $\rho=1.4$ g/cm³, $T=5000$ K (long-dashed line). The curves have been obtained by averaging over the configurations of the MD simulations.

tion (from 52 to 292, depending on the temperature) $\sigma(\omega)$ falls off artificially fast for large values of ω ; however this does not represent a serious problem for the determination of the dc electrical conductivity $\sigma(\omega=0)$. In the case of a previous application to liquid sodium¹² the electrical conductivity computed using this Kubo-Greenwood approach exhibited some discrepancies with respect to the experimental data. However, the agreement with experiment improved as a function of the temperature and was quite satisfactory at the highest temperatures (850 and 1000 K) considered.

III. RESULTS AND DISCUSSION

Figure 1 reports the pair correlation function $g(r)$ of liquid aluminum computed at the different densities considered in the present study. The effect of increasing the temperature from 1000 to 5000 K is evident. The peaks become flatter and broader. In particular, the height of the first peak decreases whereas its width increases on raising the temperature. In contrast, the effect of changing the density appears to be much smaller. Similar conclusions can be drawn by looking at the Al ion angular distribution (Fig. 2). The angle

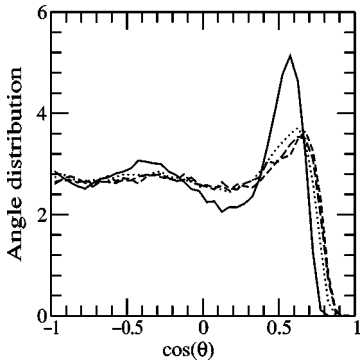


FIG. 2. Angle distribution function $g_3(\theta, r_m)$ of liquid aluminum (see text for definition) at different densities and temperatures: $\rho=2.0$ g/cm³, $T=1000$ K (solid line); $\rho=2.0$ g/cm³, $T=5000$ K (dotted line); $\rho=1.7$ g/cm³, $T=5000$ K (dashed line); $\rho=1.4$ g/cm³, $T=5000$ K (long-dashed line). The cutoff distance r_m is taken as the position of the first minimum of the corresponding $g(r)$ function.

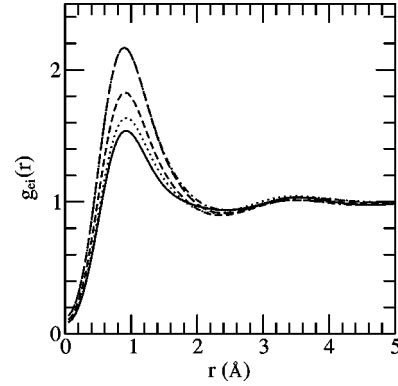


FIG. 3. Electron-ion pair correlation function $g_{ei}(r)$ of liquid aluminum at different densities and temperatures: $\rho=2.0$ g/cm³, $T=1000$ K (solid line); $\rho=2.0$ g/cm³, $T=5000$ K (dotted line); $\rho=1.7$ g/cm³, $T=5000$ K (dashed line); $\rho=1.4$ g/cm³, $T=5000$ K (long-dashed line); $\rho=1.4$ g/cm³, $T=8000$ K (dot-dashed line). The curves have been obtained by averaging over some configurations of the MD simulation.

distribution function $g_3(\theta, r_m)$ measures triplet correlations: here θ indicates the angle between the two vectors that join a central particle with two neighbors at a distance smaller than r_m , where the cutoff value r_m is taken as the position of the first minimum of the corresponding $g(r)$ function. At 1000 K the $g_3(\theta, r_m)$ function has the typical structure of liquid metals close to melting conditions and, for instance, it resembles that reported²⁶ for liquid sodium at 420 K. However, at 5000 K the structure is considerably reduced and one observes a rather broad and flat distribution.

In Fig. 3, the electron-ion pair correlation function $g_{ei}(r)$ has been plotted. This function describes the correlation between the local density of the valence electrons and the local density of the ions. As in Ref. 12 $g_{ei}(r)$ is computed according to

$$g_{ei}(r) = \frac{1}{4\pi r^2 n_0 N} \left\langle \sum_I^N \int d\mathbf{r}' n(\mathbf{r}') \delta(|\mathbf{r}' - \mathbf{R}_I| - r) \right\rangle, \quad (8)$$

where n_0 is the average density of electrons and the bracket indicates temporal average. As can be seen, the probability that the valence electronic charge is close to a given ion mainly depends on the density (the temperature dependence is small for $\rho=2.0$ g/cm³ and almost negligible for $\rho=1.4$ g/cm³, in this latter case the curves corresponding to $T=5000$ and $T=8000$ K are almost coincident) and increases as the density decreases. Although this certainly reflects an increasing electron charge localization, no dramatic effect, suggesting the onset of a metal-insulator transition, is observed.

In Fig. 4 the electronic density of states (EDOS) is reported (data have been averaged over 10 uncorrelated MD configurations and on energy intervals of width 0.3 eV). As can be seen, at all the temperatures and density considered, EDOS clearly exhibits a metallic behavior: neither an energy gap nor a minimum appears in EDOS, which could reveal the occurrence of a metal-insulator transition. The absence of such a transition is confirmed by the analysis of the electrical conductivity data. As discussed in Sec. II, using the Kubo-

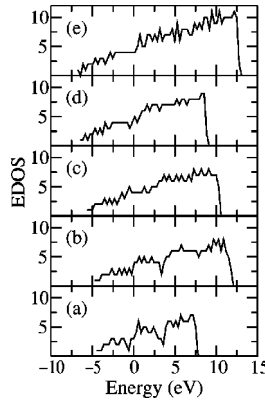


FIG. 4. Electronic density of states, EDOS, of liquid aluminum: (a) $\rho=2.0$ g/cm³, $T=1000$ K; (b) $\rho=2.0$ g/cm³, $T=5000$ K; (c) $\rho=1.7$ g/cm³, $T=5000$ K; (d) $\rho=1.4$ g/cm³, $T=5000$ K; (e) $\rho=1.4$ g/cm³, $T=8000$ K. Data have been averaged over 10 uncorrelated MD configurations and on energy intervals of width 0.3 eV.

Greenwood approach, the dc electrical conductivity $\sigma(\omega=0)$ has to be calculated by extrapolating the optical conductivity expression for finite ω . This is not trivial since in finite systems the energy levels are always discrete (even in a metal the energy-band gap is not exactly zero) so that $\sigma(\omega)$ unphysically falls to zero for very small values of ω . Therefore, it is more convenient to estimate σ by assuming a given functional form for $\sigma(\omega)$, checking whether it fits well the calculated data, and then computing its zero-frequency limit. In Fig. 5 the behavior of the frequency-dependent conductivity $\sigma(\omega)$ is reported in “raw” data form and fitted to a Drude function (obviously the frequency interval used for the fit is limited by the number of computed excited states - see Sec. II). Data have been obtained by averaging over 10 uncorrelated ionic configurations of the MD simulations. Both σ and the relaxation time τ have been fitted using the Drude formula

$$\sigma(\omega) = \frac{\sigma}{1 + \omega^2 \tau^2}. \quad (9)$$

As can be seen from Fig. 5, the Drude function provides a good fit to the simulation data for all the densities and temperatures considered. Note that, in the present study, in contrast to the work of Mostovych and Chan,¹ the Drude behavior is not assumed *a priori*. The resulting σ and τ parameters, obtained by the fitting procedure, can be found in Table III. Both σ and τ decrease by decreasing the density and increasing the temperature.

TABLE III. Drude parameters (dc electrical conductivity σ , relaxation time τ , and plasma frequency ω_p) obtained by fitting the optical conductivity curves of Fig. 5, in the range 0–2.6 eV for $T=1000$ K, $\rho=2.0$ g/cm³, and 0–3.8 eV for the other cases.

ρ (g/cm ³)	T (K)	σ ($10^3(\Omega \text{ cm})^{-1}$)	τ (10^{-16} s)	ω_p (eV)
2.0	1000	30.4	6.2	15.5
2.0	5000	25.4	5.4	15.1
1.7	5000	17.2	4.4	13.8
1.4	5000	10.5	3.3	12.6
1.4	8000	9.3	2.8	12.6

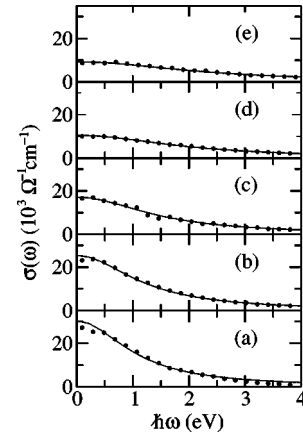


FIG. 5. Optical conductivity $\sigma(\omega)$ of liquid aluminum, obtained by averaging over 10 uncorrelated configurations of the MD simulation: (a) $\rho=2.0$ g/cm³, $T=1000$ K; (b) $\rho=2.0$ g/cm³, $T=5000$ K; (c) $\rho=1.7$ g/cm³, $T=5000$ K; (d) $\rho=1.4$ g/cm³, $T=5000$ K; (e) $\rho=1.4$ g/cm³, $T=8000$ K. The circles have been obtained by direct calculation (the size of the statistical errors is comparable with that of the symbols), while the lines are the Drude-curve fits.

Concerning the effect that a more thorough sampling of the BZ has on the estimated values of σ , one expects (and this is confirmed by the following results) that, at the relatively high temperatures considered in the present simulations, it is not dramatic. In fact, as it has been shown in Ref. 12, by increasing the temperature, the resulting broadening of the Fermi function lowers the energy resolution needed and therefore a coarser k -point sampling suffices. In order to verify this expectation, at all the densities considered, and at $T=1000$ and 5000 K, the $\sigma(\omega)$ function, computed using the Γ -point only sampling of the BZ, has been compared with that obtained from a much more expensive calculation with 8 k points (see Fig. 6). Since a single ionic configuration was used, relatively large fluctuations are present (particularly at 1000 K), however it is evident that the difference between the values of σ obtained with the two different samplings is substantial only at $T=1000$ K, and decreases by increasing the temperature. For $T=1000$ K the effect of using the 8 k -point sampling of the BZ, instead of the Γ -point sampling, is similar to that observed,¹² at the same temperature, in the *ab initio* simulation of liquid sodium.

The behavior of the computed σ is plotted in Fig. 7, where it is compared with the results of other theoretical calculations and with the data reported by Mostovych and Chan.¹ Note that, at the fixed temperature of 5000 K, the dc

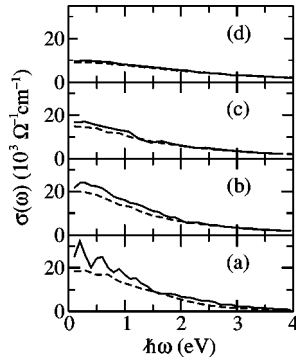


FIG. 6. Optical conductivity $\sigma(\omega)$ of liquid aluminum, obtained by considering a single MD configuration: (a) $\rho=2.0$ g/cm³, $T=1000$ K; (b) $\rho=2.0$ g/cm³, $T=5000$ K; (c) $\rho=1.7$ g/cm³, $T=5000$ K; (d) $\rho=1.4$ g/cm³, $T=5000$ K. The solid and dashed lines connect data obtained using the Γ -point sampling of the BZ and the 8 k -vector sampling, respectively.

electrical conductivity decreases approximately linearly with the density, in agreement with all the conductivity models;²⁵ however, given the small number of points computed and the size of the errors affecting the determination of σ it is not possible to have a precise estimate of the power law. The σ values computed by the simulation appear to be intermediate between those extrapolated from liquid metal data,²⁷ obtained near the melting point using a Ziman approach, and those computed by the model of Perrot and Dharma-wardana.⁴ Note that the different theoretical evaluations tend to be closer to one another as the density decreases.

In contrast, in their experiment, Mostovych and Chan¹ found that, although at low temperatures ($T < 4000$ K ~ 0.35 eV), note that the uncertainty in the temperature measurements is estimated¹ to be about ± 600 K $\sim \pm 0.05$ eV) their conductivity is in agreement with standard liquid metal Ziman-type calculations²⁷ and lies on the curve extrapolated from tabulated conductivities of liquid aluminum from near the melting point,²⁸ at higher temperatures the conductivity falls sharply and enters a region associated with a minimum metallic conductivity and the metal-insulator transition.² While it is easy to distinguish a conductor from an insulator at zero temperature (the former has a finite value of σ , for the latter $\sigma=0$), in a fluid phase at finite T such a distinction is less rigorous and must be based on the magnitude of σ . For aluminum the metal-non metal borderline can be placed at about 2500-3000 ($\Omega \text{ cm}$)⁻¹ (see Ref. 1). Given the approximations involved in the determination of σ (extrapolation to zero frequency by the Drude fit, finite size of the supercell with the Γ point only sampling of the BZ, use of DFT-LDA eigenvalues and eigenstates, ...) the present results can be affected by an uncertainty as large as 20-30%. However, even taking these margins of uncertainty into account, it is evident that the electrical conductivity computed by *ab initio* simulation always remains much higher (at least a factor 3) than the minimum metallic conductivity level. Moreover, by decreasing the density and increasing the temperature no dramatic electrical conductivity falling is observed. Rather the σ decrease is quite smooth. Therefore, the present data do not support the existence of a metal-insulator transition in the range of physical parameters

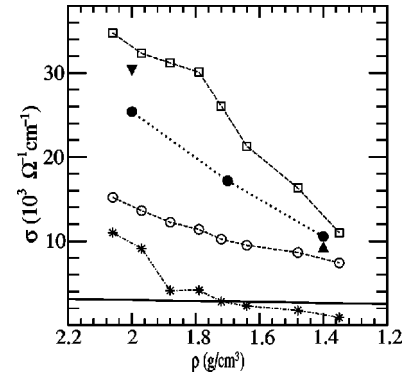


FIG. 7. DC electrical conductivity of liquid aluminum, as a function of the density, obtained by the simulations (solid triangle down for $T=1000$ K, solid circles for $T=5000$ K, and solid triangle up for $T=8000$ K) compared with the results reported by Mostovych and Chan (Ref. 1) (stars), and theoretical calculations (data have been taken from Fig. 4 of Ref. 1) performed by extrapolating from liquid metal data near the melting point (open circles) and using the model of Perrot and Dharma-wardana (Ref. 4) (open squares), respectively. Data are represented by symbols, while the lines are just a guide for the eye. The solid line indicates the minimum metallic conductivity level.

considered. Instead the system behavior seems to be consistent with that of a standard liquid metal, in qualitative agreement with other theoretical calculations.

IV. CONCLUSIONS

In conclusion, I have presented a calculation of structural and electronic properties of dense hot aluminum using finite-temperature *ab initio* MD simulation. The system has been studied at densities and temperatures corresponding to those measured in the recent laser-heating experiment of Mostovych and Chan.¹ In the present calculation, the electrical conductivity has been computed using the Kubo-Greenwood formulation that transcends the limitations of the Ziman approach. The simulation results do not support the conclusions of Mostovych and Chan¹ about the existence of a metal-insulator transition characterized by a dramatic decrease of the electrical conductivity.

I am aware of the limitations of the present simulation that, besides those related to the practical calculation of σ using the Kubo-Greenwood formula with DFT-LDA eigenstates and eigenvalues, are also in terms of both size and time scale. For instance, in a small system, large wavelength ionic fluctuations are suppressed by the periodic boundary conditions, and therefore the associated contribution to the electrical conductivity is neglected. However, these limitations are only expected to have quantitative, not qualitative effects on the calculations. Since also the experimental results of Mostovych and Chan are affected by relatively large margins of uncertainty, due to the approximations used in the data interpretation and particularly in extrapolating the electrical conductivity values, it would be very appropriate if the electronic properties of dense hot aluminum could be further investigated in other experiments.

Note added in proof. After acceptance of this paper an experimental study was published [J. F. Benage, W. R. Shanahan, and M. S. Murillo, Phys. Rev. Lett. **83**, 2953 (1999)] in which direct measurements of the electrical conductivity

in dense hot aluminum have been carried out. The results of this study (particularly at the lowest temperatures) are in qualitative agreement with those presented here and support the conclusions drawn in the present paper.

-
- ¹A. N. Mostovych and Y. Chan, Phys. Rev. Lett. **79**, 5094 (1997).
²N. F. Mott, *Metal-Insulator Transitions* (Taylor & Francis, New York, 1990).
³G. A. Rinker, Phys. Rev. B **31**, 4207 (1985); Phys. Rev. A **37**, 1284 (1988).
⁴F. Perrot and M. W. C. Dharma-wardana, Phys. Rev. A **36**, 238 (1987); Phys. Rev. E **52**, 5352 (1995).
⁵S. Tanaka, X. Yan, and S. Ichimaru, Phys. Rev. A **41**, 5616 (1990); H. Kitamura and S. Ichimaru, Phys. Rev. E **51**, 6004 (1995).
⁶D. E. Logan, I. J. Bush, and P. A. Madden, Z. Phys. Chem. **184**, 25 (1994).
⁷R. Kubo, J. Phys. Soc. Jpn. **12**, 570 (1957); D. A. Greenwood, Proc. Phys. Soc. **71**, 585 (1958).
⁸A. Alavi, J. Kohanoff, M. Parrinello, and D. Frenkel, Phys. Rev. Lett. **73**, 2599 (1994).
⁹N. D. Mermin, Phys. Rev. **137**, A1441 (1965).
¹⁰I used the finite temperature *ab initio* MD code of A. Alavi and T. Deutsch, built from the code CPMD, version 3.0, developed by J. Hutter, P. Ballone, M. Bernasconi, P. Focher, E. Fois, S. Goedecker, M. Parrinello, M. Tuckerman, at MPI für Festkörperforschung and IBM Zurich Research Laboratory (1990-1997).
¹¹A. Alavi, M. Parrinello, and D. Frenkel, Science **269**, 1252 (1995).
¹²P. L. Silvestrelli, A. Alavi, and M. Parrinello, Phys. Rev. B **55**, 15 515 (1997).
¹³P. L. Silvestrelli, A. Alavi, M. Parrinello, and D. Frenkel, Europhys. Lett. **33**, 551 (1996); Phys. Rev. B **53**, 12 750 (1996).
¹⁴P. L. Silvestrelli, A. Alavi, M. Parrinello, and D. Frenkel, Phys. Rev. Lett. **77**, 3149 (1996); Phys. Rev. B **56**, 3806 (1997).
¹⁵P. L. Silvestrelli and M. Parrinello, J. Appl. Phys. **83**, 2478 (1998).
¹⁶A. Alavi, P. Hu, T. Deutsch, P. L. Silvestrelli, and J. Hutter, Phys. Rev. Lett. **80**, 3650 (1998).
¹⁷N. Troullier and J. L. Martins, Phys. Rev. B **43**, 1993 (1991).
¹⁸P. E. Blöchl and M. Parrinello, Phys. Rev. B **45**, 9413 (1992).
¹⁹M. F. Cai, T. P. Djugan, and V. E. Bondybey, Chem. Phys. Lett. **155**, 430 (1989).
²⁰F. Perrot and M. W. C. Dharma-wardana, Phys. Rev. A **30**, 2619 (1984); D. G. Kanhere, P. V. Panat, A. K. Rajagopal, and J. Callaway, *ibid.* **33**, 490 (1986).
²¹W. T. Pollard and R. A. Friesner, J. Chem. Phys. **99**, 6742 (1993).
²²H. J. Monkhorst and J. D. Pack, Phys. Rev. B **13**, 5188 (1976).
²³J. M. Ziman, Philos. Mag. **6**, 1013 (1961).
²⁴R. Car and M. Parrinello, Phys. Rev. Lett. **55**, 2471 (1985).
²⁵O. Pfaffenzeller and D. Hohl, J. Phys.: Condens. Matter **9**, 11 023 (1997).
²⁶G.-X. Qian, M. Weinert, G. W. Fernando, and J. W. Davenport, Phys. Rev. Lett. **64**, 1146 (1990).
²⁷N. W. Ashcroft and J. Lekner, Phys. Rev. **145**, 83 (1966).
²⁸Melting of aluminum at ambient pressure occurs at $\rho = 2.37 \text{ g/cm}^3$ and $T = 933 \text{ K}$, with a σ conductivity of $41 \times 10^3 \text{ } (\Omega \text{ cm})^{-1}$.